

Optical conductivity of the non-superconducting cuprate $\text{La}_{8-x}\text{Sr}_x\text{Cu}_8\text{O}_{20}$

A. Lucarelli, S. Lupi, P. Calvani, and P. Maselli

Istituto Nazionale di Fisica della Materia - Dipartimento di Fisica, Università di Roma La Sapienza, Piazzale Aldo Moro 2, I-00185 Roma, Italy

G. De Marzi and P. Roy

Laboratoire pour l'Utilisation du Rayonnement Electromagnétique, Université Paris-Sud, 91405 Orsay, France

N. L. Saini and A. Bianconi

Istituto Nazionale di Fisica della Materia - Dipartimento di Fisica, Università di Roma La Sapienza, Piazzale Aldo Moro 2, I-00185 Roma, Italy

T. Ito and K. Oka

Electrotechnical Laboratory, 1-1-1 Umezono, Tsukuba, Ibaraki 305-8568, Japan
 (December 2, 2024)

Abstract

$\text{La}_{8-x}\text{Sr}_x\text{Cu}_8\text{O}_{20}$ is a non-superconducting cuprate, which exhibits a doubling of the elementary cell along the c axis. Its optical conductivity $\sigma(\omega)$ has been first measured here, down to 20 K, in two single crystals with $x = 1.56$ and $x = 2.24$. Along c $\sigma(\omega)$ shows, in both samples, bands due to strongly bound charges, thus confirming that the cell doubling is due to charge ordering. In the ab plane, in addition to the Drude term one observes an infrared peak at ~ 0.1 eV and a midinfrared band at 0.7 eV. The 0.1 eV peak hardens considerably below 200 K, in correspondence of an anomalous increase in the sample dc resistivity, in agreement with its polaronic origin. This study allows one to establish relevant similarities and differences with respect to the spectrum of the ab plane of the superconducting cuprates.

PACS numbers: 74.25.Gz, 74.72.-h, 74.25.Kc

I. INTRODUCTION

In recent years, several studies have been devoted to the problem of localization and ordering of the doped charges in the cuprates. Theories of their metallic phase in terms of fluctuating charged stripes^{1–4} have been proposed. Models of high- T_c superconductivity^{5–7} have also been proposed, which assume a coexistence of free and bound charges. Experimentally, charged superlattices have been clearly detected by diffraction techniques in compounds⁸ like $\text{La}_{2-x}\text{Sr}_x\text{NiO}_4$ or $\text{La}_{2-x}\text{Sr}_x\text{MnO}_4$, that are isostructural to $\text{La}_{2-x}\text{Sr}_x\text{CuO}_4$ (2-1-4). In this latter however, ordered arrays of spin and charge have been observed only upon partial replacement of La by Nd.⁹ On the other hand, charged stripe fluctuations have been detected in $\text{YBaCu}_3\text{O}_{7-x}$ by use of neutron scattering¹⁰ and ion channeling¹¹ as well as, in 2-1-4, by X-ray absorption¹² and angle-resolved photoemission.¹³

When considering the optical spectra, it is well known that the *ab*-plane optical conductivity $\sigma(\omega)$ of a metallic cuprate does not follow a normal Drude behavior.^{14,15} Moreover, bands indicating the existence of selftrapped carriers have been directly resolved in several cuprates.^{16,23,24,20} In general, the infrared conductivity

$$\sigma(\omega) = \frac{\omega}{4\pi} \text{Im}[\tilde{\epsilon}], \quad (1)$$

can be fitted by use of a Drude-Lorentz dielectric function

$$\tilde{\epsilon} = \epsilon_\infty - \frac{\omega_D^2}{\omega^2 - i\omega\Gamma_D} + \sum_j \frac{S_j^2}{(\omega^2 - \omega_j^2) - i\omega\Gamma_j}, \quad (2)$$

where in the sum two oscillators correspond to the so-called *d* band and to the midinfrared (MIR) band. This analysis is supported by the fact that both of them are directly resolved in the spectra of the doped cuprates below the insulator-to-metal (IMT) transition.¹⁶ Two other oscillators are often needed to reproduce the Cu-O charge-transfer band which appears in the near- infrared and the visible.¹⁷

The *d*-band is observed at $\omega_d \sim 0.1$ eV in both lightly doped $\text{La}_2\text{CuO}_{4+y}$,¹⁸ and $\text{Nd}_2\text{CuO}_{4-y}$,^{16,19} and is extremely sensitive to both doping and temperature. In $\text{Nd}_{2-x}\text{Ce}_x\text{CuO}_{4-y}$,²⁰ it increases in intensity and displaces towards lower energies for both increasing doping and lowering temperature.²⁰ The softening of an infrared band for $T \rightarrow 0$ is quite unusual as it will be shown here also, and allows one to make interesting comparisons with the non-superconducting oxides. This contribution is still observed at $x \simeq 0.15$, where $\text{Nd}_{2-x}\text{Ce}_x\text{CuO}_{4-y}$ is superconducting at optimum doping, at frequencies even lower than the softest transverse phonon mode.^{20,21} Finally it disappears in the normal metallic phase at high doping ($x > 0.18$). Its presence in superconducting cuprates, at least those with low T_c , is confirmed by recent observations on superconducting $\text{Bi}_2\text{Sr}_2\text{CuO}_6$ close to optimum doping ($T_c = 20$ K).²²

The above observations are explained by assuming that the *d* band is due to polaronic charges, that increasingly selftrap at low T due to the competition between thermal excitations and charge- lattice interaction.^{16,18,20,23,24} The softening of the charge binding energy for increasing polaron density (i.e. for increasing doping and/or decreasing temperature) is explained in terms of polaron-polaron interactions.^{25–28} The strength of the *d* band seems also to increase as the dimensionality of the environment decreases. In $\text{YBa}_2\text{Cu}_4\text{O}_8$, an

untwinned cuprate of the YBCO family that has both conducting Cu-O planes and Cu-O chains, the optical conductivity shows a Drude contribution well distinguished from a huge polaronic peak at 0.1 eV, when the radiation field is directed along the chains.²⁹ In turn, the nearly T -independent midinfrared band (MIR) has been observed both in layered and cubic perovskites, upon doping, at ≈ 0.5 eV.^{17,30,31} This band, which close to the MIT transition helps to build up the Drude term with part of its spectral weight,^{17,30,31} is usually attributed to electronic states created by doping in the Cu-O charge-transfer gap.

In the present paper the optical properties of $\text{La}_{8-x}\text{Sr}_x\text{Cu}_8\text{O}_{20}$ (8-8-20) will be studied, and analyzed by using the model of Eq. 2. $\text{La}_{8-x}\text{Sr}_x\text{Cu}_8\text{O}_{20}$ contains the same chemical species as the 40 K superconductor 2-1-4. However, i) it is not superconducting for any x ; ii) it exhibits in the electron diffraction spectra well defined superlattice spots for $x \sim 1.6$, indicating unit-cell doubling along the c axis, diffused spots for ~ 2.2 .³² Therefore, an infrared study of 8-8-20 can add information on the ordering process that takes place in this cuprate and provide interesting comparisons with the optical behavior of the superconducting cuprates.

II. SAMPLE DESCRIPTION AND EXPERIMENTAL PROCEDURE

The crystal structure of $\text{La}_{8-x}\text{Sr}_x\text{Cu}_8\text{O}_{20}$ is tetragonal,³³ with lattice constants $a_0 = b_0 = 1.084$ nm, $c_0 = 0.3861$ nm. It can be derived from that of $\text{La}_{2-x}\text{Sr}_x\text{CuO}_4$ (2-1-4) by eliminating oxygen ions in a regular way. As a result, one is left with corner-sharing Cu-O₆ octahedra, Cu-O₅ pyramids and Cu-O₄ squares. The latters form one-dimensional (1D) chains along the c axis, while the corner-sharing Cu-O₆ octahedra and the Cu-O₅ pyramids form a three-dimensional (3D) network of essentially 1D paths. The charges travel along this network and there are no Cu-O conducting sheets. The transport properties of $\text{La}_{8-x}\text{Sr}_x\text{Cu}_8\text{O}_{20}$ have been investigated on single crystals with $1.56 < x < 2.24$. In this range the nominal charge varies from 0.2 to 0.3 holes per Cu atom, compared with 0.06 to 0.3 holes per Cu atom in the metallic phase of $\text{La}_{2-x}\text{Sr}_x\text{CuO}_4$. Resistivity measurements on single crystals showed that 8-8-20, similarly to other cuprates, has an "anomalous" metallic region for $1.5 \lesssim x \lesssim 1.8$, followed by a normal metallic phase for $x \gtrsim 2$; however, for any x , it is not superconducting down to 1.3 K.³⁴ At room temperature the anisotropy in the resistivity is $\rho_c/\rho_{ab} \sim 10$ at any x . At constant temperature, both ρ_{ab} and ρ_c decrease for increasing x , as usually observed in doped Mott insulators. As a function of T , both ρ_{ab} and ρ_c are metallic-like in the whole doping range, but exhibit an anomalous broad maximum³⁵ between two temperatures T_{c1} and T_{c2} (with $T_{c1} > T_{c2}$) which change with x . T_{c1} has been associated with a reduction in the scattering rate of the itinerant holes, related to a weak ferromagnetic ordering in the 3D network. Below T_{c2} an antiferromagnetic (AFM) order is observed, and attributed to the chains of Cu-O₄ squares aligned along the c axis.³⁴ The AFM transition is associated with strong, opposite variations of the Hall coefficients R_H in the ab plane and along the c axis, and also with a sudden change in ρ_{ab} . These effects have been explained with the formation of a gap at the Fermi surface along certain directions, due to the formation of spin density waves at T_{c2} .³⁵ Both T_{c1} and T_{c2} decrease by increasing x , until a conventional metallic behavior is established in the sample with $x=2.24$.³⁵ As already mentioned, electron diffraction studies³⁴ have shown that an ordering process causes a doubling of the elementary cell along the c direction. According to the

authors, the ordering involves the charges introduced by doping, most probably in the CuO_4 squares. Indeed, one may remark that the anomalies in the resistivity of 8-8-20 are quite similar to those detected in compounds like NbSe_3 , where one-dimensional charge density waves form below a critical temperature.³⁶

The two single crystals selected for the present optical study of $\text{La}_{8-x}\text{Sr}_x\text{Cu}_8\text{O}_{20}$ have $x = 2.24$ and $x = 1.56$, the highest and nearly the lowest doping level, respectively, that have been studied in the literature. Basing on the transport properties³⁴ of crystals obtained from the same batch, the former should provide a good metallic spectrum for reference and the latter, which has $T_{c1} = 145$ K and $T_{c2} = 85$ K, is expected to exhibit 'anomalous' spectral features in the clearest way. Both crystals were grown by the travelling- solvent floating zone method.³⁵ Their chemical composition was determined by the inductively coupled plasma atomic emission (ICP-AES). The transport and magnetic properties of the samples have been described in Ref. 35.

The samples were mounted on the cold finger of a two stage closed- cycle cryostat, whose temperature was kept constant within 2 K and could be varied from 295 to 20 K. The reflectance $R(\omega)$ of the samples, with the radiation field in the ab plane, was measured relative to gold- and aluminum-plated references. With the radiation field polarized along the c axis, the reference was obtained by evaporating directly gold on the sample.³⁷ Thus we obtained reliable absolute values of the reflectivity in spite of the small transverse dimension of the sample. The spectra were collected by a rapid scanning interferometer, typically from 80 cm^{-1} to 20000 cm^{-1} . A Drude-Lorentz fit was used to extrapolate the reflectivity to $\omega = 0$. On the high-energy side, our data were extrapolated with the reflectivity reported in Ref. 38 for $\text{La}_{2-x}\text{Sr}_x\text{CuO}_4$, under the reasonable assumption that the ultraviolet bands of 8-8-20 are not too different from those of 2- 1-4. The real part of the optical conductivity $\sigma(\omega)$ was then extracted from $R(\omega)$ by usual Kramers-Kronig trasformations.

III. RESULTS AND DISCUSSION

A. Optical response of the c axis

The reflectivity $R(\omega)$ measured along the c axis of $\text{La}_{8-x}\text{Sr}_x\text{Cu}_8\text{O}_{20}$ is shown in Fig. 2 for $x = 2.24$ (top) and $x = 1.56$ (bottom). The spectra are reported in the range from 40 to 20000 cm^{-1} at four different temperatures. $R(\omega)$ exhibits a metallic-like behavior in both samples with a well evident pseudo-plasma edge around 10000 cm^{-1} . The electronic band in the visible range is similar to features observed in most cuprates^{17,30} and attributed to the Cu-O charge-transfer transitions. For $x = 2.24$, it can be reproduced by two Lorentzians placed at 17800 and 21200 cm^{-1} , with $\epsilon_\infty = 4.1$. At low frequency $R(\omega)$ differs in the two crystals. The sample with $x = 2.24$ shows a standard metallic reflectivity, except for a smooth anomaly at $\sim 600 \text{ cm}^{-1}$ for $T \lesssim 150$ K. On the other hand, for $x = 1.56$ there is a clear change of slope in $R(\omega)$ around 300 cm^{-1} , suggestive of two different contributions to $\sigma(\omega)$. The contribution at high frequency exhibits a more pronounced temperature dependence than that at low frequency.

The multi-component structure of the absorption is quite evident in the real part of the optical conductivity, reported for both crystals in Fig. 3. In the sample with $x = 2.24$ (top), $\sigma(\omega)$ exhibits two well-defined components in the infrared, with different temperature

behaviors: a Drude term which is dominating for $\omega \lesssim 1500 \text{ cm}^{-1}$ and narrows for $T \rightarrow 0$, and a broad band in the midinfrared. This latter is separated from the Drude contribution by a change of slope at $\sim 1500 \text{ cm}^{-1}$, more pronounced at low T . The inset compares the experimental $\sigma(\omega)$ at 20 K with a fit to Eq. 2. In the frequency range shown in the inset, this includes a Drude term with $\omega_p \simeq 1500 \text{ cm}^{-1}$ at all temperatures and a Γ_D which decreases from 1200 cm^{-1} at 295 K to 400 cm^{-1} at 20 K, a contribution in the midinfrared peaked at 2300 cm^{-1} at 20 K, and a weak background centered at about 9000 cm^{-1} . Basing on these results, it seems quite reasonable to assign the midinfrared band to those bound charges which produce a diffuse scattering in the electron diffraction spectra of the $x = 2.24$ sample. In turn, the strong Drude term accounts for the good dc conductivity of this compound along the c axis. Therefore the present data show a coexistence of free and bound charges in the cuprate even at $x = 2.24$, a doping value which provides at all temperatures the lowest dc resistivity reached by this compound.

A Drude-like absorption and a band in the midinfrared are found also in the sample with $x = 1.56$ (bottom panel of Fig. 3) where, however, they are directly resolved in the $\sigma(\omega)$. This is due to the fact that the Drude term is weaker than at $x = 2.24$ by a factor of 10, the midinfrared band by a factor of 2. By recalling the results of ref. 35, one may assign the sharp, T -dependent midinfrared band here observed for $x = 1.56$ to the photoexcitation of those bound charges which, for $x = 1.6$, contribute sharp superlattice spots to the electron-diffraction spectra. The peak frequency increases monotonically from $\sim 2300 \text{ cm}^{-1}$ at 295 K to $\sim 3300 \text{ cm}^{-1}$ at 20 K. At the latter temperature, the corresponding band in the inset of Fig. 3) is peaked at $\sim 2000 \text{ cm}^{-1}$. As already mentioned, a softening of the bound-charge absorption for increasing doping has also been observed in superconducting families of cuprates.²⁰ If one describes the bound charges in terms of small polarons, as previously done for other perovskites with charge ordering,^{39,40} the peak energy of the band is just twice the charge-lattice binding energy E_p .⁴¹ From Fig. 3, at $x = 1.56$ one thus finds $E_p \sim 1100 \text{ cm}^{-1}$ at 295 K, $E_p \sim 1600 \text{ cm}^{-1}$ at 20 K.

The full opening of a charge-ordering gap in $\sigma(\omega)$, as observed for instance⁴⁰ in $\text{La}_{1.67}\text{Sr}_{0.33}\text{NiO}_4$, is prevented in $\text{La}_{6.44}\text{Sr}_{1.56}\text{Cu}_8\text{O}_{20}$ by the Drude-like component, which in Fig. 3 is observed at any temperature. This shows that the bound charges are coexisting with free charges in the 1.56 crystal, consistently with its not negligible dc conductivity. Due to the peculiar structure of 8-8-20 along the c axis, the two types of charges are likely to be even spatially separated. The ordered charges can occupy the CuO_4 chains, as already proposed,³⁴ while the free carriers may travel along the zig-zag paths formed by the polyhedral network, which are aligned in average along the c direction. A similar situation is encountered for instance in NbSe_3 , which remains metallic down to the lowest temperatures in spite of the formation of charge-density waves. These latters appear in two out of the three infinite-length trigonal prisms that build up the structure of NbSe_3 , while the third one remains metallic.⁴²

B. Optical response of the ab plane

The reflectivity $R(\omega)$ of the ab plane of $\text{La}_{8-x}\text{Sr}_x\text{Cu}_8\text{O}_{20}$ is shown in Fig. 4 for $x = 2.24$ (top) and $x = 1.56$ (bottom). The spectra are reported in the range from 80 to 3000 cm^{-1} at different temperatures. In the insets of both figures $R(\omega)$ is shown at two temperatures

in the energy range from 80 to 20000 cm⁻¹. $R(\omega)$ presents a metallic-like behavior in both samples with a well evident pseudo-plasma edge around 10000 cm⁻¹. However, below 3000 cm⁻¹ the reflectivity of the sample with $x = 2.24$ (top panel) increases steadily by lowering the temperature according to a conventional metallic behavior, while in the sample with $x = 1.56$ (bottom panel) $R(\omega)$ has a more complicated behavior. Indeed, by lowering T the reflectivity first increases down to 250 K, then it decreases to reach at 20 K its minimum value.

The real part $\sigma(\omega)$ of the optical conductivity is shown in Fig. 5 for both samples, between 80 and 5000 cm⁻¹ and at different temperatures. In both insets, $\sigma(\omega)$ is shown at two temperatures in the whole energy range. In the sample with $x = 2.24$ (top panel) $\sigma(\omega)$ exhibits a conventional metallic behavior. Indeed, a best fit to Eq. 2 gives good results by using the Drude term only. The plasma frequency (5500 cm⁻¹) is approximately independent of temperature, while Γ_D decreases from 250 cm⁻¹ at 295 K to 90 cm⁻¹ at 20 K.

On the other hand, in the sample with $x = 1.56$ (bottom panel), where the anomalies in the dc properties are most evident, $\sigma(\omega)$ exhibits a complex structure where at least four absorption bands are observed. The one at the highest energy is a broad absorption located around 15000 cm⁻¹, independent of T , which may be assigned to the charge transfer transition between Cu and O. A second well-evident absorption is observed around 6000 cm⁻¹ and is nearly independent of temperature. This feature is then different from the midinfrared bands observed along the c axis and assigned to bound charges. It is instead similar to the mid-infrared band (MIR) observed in most HCTS.^{30,17} According to a pseudo-potential calculation⁴³ of the electronic structure of La₄BaCu₅O₁₃, a compound with lattice structure and transport properties similar to those of La_{8-x}Sr_xCu₈O₂₀, the MIR band is due to a transition from an electronic band located at ~ 0.5 eV below the Fermi energy E_F to a band which crosses E_F .

A third absorption in the bottom panel of Fig. 5 is strongly dependent on T and extends from ~ 500 to ~ 4000 cm⁻¹. At low temperature it is separated from the T -independent MIR band by a broad minimum centered at about 3000 cm⁻¹ (see also the inset). Its intensity increases from 295 K to 250 K to decrease gradually from 250 to 20 K. Let us name its peak frequency ω_d , as for the other cuprates mentioned in the Introduction, where the corresponding band is assigned to the photoexcitation of polaronic charges.^{29,18,24,20} In the present La_{6.44}Sr_{1.56}Cu₈O₂₀ crystal ω_d remains constant at ~ 800 cm⁻¹ between 295 and 200 K, but at lower temperatures it hardens considerably and reaches about 1500 cm⁻¹ at 20 K. This behavior with temperature is quite different from that of superconducting cuprates, where ω_d softens for $T \rightarrow 0$, and is related to that of the dc resistivity of the same sample. This is shown in Fig. 6. In the inset of the Figure, the ab -plane resistivity the raw ρ_{ab} data are reported for both crystals as solid lines here considered.³⁵ At $x = 1.56$ ρ_{ab} is larger than for the $x = 2.24$ sample, which behaves approximately like a standard metal. However, if one scales the ρ_{ab} of this latter by a normalizing constant factor (dashed line), the two curves show the same temperature dependence between 295 and 200 K. On the other hand, below 200 K, ρ_{ab} for $x = 1.56$ deviates significantly upwards from the normal metallic behavior of $x = 2.24$. In the main Figure, the solid line gives $\Delta\rho_{ab}/\rho_{ab} = [\rho_{ab}(1.56) - \rho_{ab}(2.24)]/\rho_{ab}(2.24)$, namely the deviation of ρ_{ab} in the $x = 1.56$ sample from a normal metallic behavior. The dots represent in turn $\Delta\omega_d/\omega_d = [\omega_d(T) - \omega_d(295)]/\omega_d(295)$, namely the relative "blue shift" of the d band with respect to its room-temperature value.

Figure 6 shows a clear correlation between the temperature behavior of $\Delta\rho_{ab}/\rho_{ab}$ and that of $\Delta\omega_d/\omega_d$ which, one should remark, refers to a contribution at finite energy, well distinguished from the Drude term. Above 200 K, both quantities are negligibly small. Below 200 K, when the d band begins to shift towards higher energies, the resistivity starts increasing with respect to a normal metallic behavior. At the lowest T , the relative resistivity deviation attains about 40%, while the "blue shift" of the d band is nearly 100%. This observation strongly supports the polaronic interpretation of the d band in this cuprate. Indeed, according to any polaronic model of $\sigma(\omega)$, $\omega_d \propto E_p$, the selftrapping energy of the carrier. Therefore, the observed "blue shift" is predicted to produce a lower carrier mobility, in agreement with the dc observation.

One can also easily check that the displacement of the d band occurs via a transfer of spectral weight within the low- energy excitation spectrum of the carriers. Indeed, as one can see in the bottom panel of Fig. 5, $\sigma(\omega)$ is independent of T both at about 1700 cm^{-1} , and at 5000 cm^{-1} . If now one considers the effective number of carriers

$$n_{eff}(\omega_1) = \frac{2m^*V}{\pi e^2} \int_0^{\omega_1} \sigma(\omega) d\omega. \quad (3)$$

where V is the cell volume, m^* is assumed to be equal to the free electron mass, and one selects $\omega_1 = 5000\text{ cm}^{-1}$, one obtains $n_{eff}(5000) = 1.15 \pm 0.02$ at any T from 295 K to 20K. Therefore, as T changes, spectral weight is transferred across the fixed point at 1700 cm^{-1} with no contribution from the electronic transitions at higher energies.

Finally, below 500 cm^{-1} the ab -plane infrared conductivity of both samples shows a Drude-like free-particle absorption. Phonon-like peaks are superimposed to it, more clearly for $x = 1.56$ due to a reduced screening action of the carriers. The extrapolations of $\sigma(\omega)$ to $\omega = 0$ at different temperatures agree within a factor of 2 with the corresponding values of σ_{dc} extracted from the resistivities of Fig. 5.

IV. CONCLUSION

We have studied the optical properties of $\text{La}_{8-x}\text{Sr}_x\text{Cu}_8\text{O}_{20}$, a non-superconducting cuprate characterized by a network of essentially one-dimensional paths. The two single crystals here examined have $x = 1.56$ and $x = 2.24$, or approximately the lowest and highest doping, respectively, that have been studied in the literature for this compound.

We have first determined the optical response of the c axis, where previous electron-diffraction experiments on $\text{La}_{8-x}\text{Sr}_x\text{Cu}_8\text{O}_{20}$ showed clear superlattice spots for $x = 1.6$, diffuse superlattice scattering for $x = 2.24$. In the optical spectra, for $x = 1.56$ we find a strong and T -dependent midinfrared band accompanied by a weak Drude term. At $x = 2.24$ we observe a broad, nearly T - independent, midinfrared background coexisting with a strong and narrow Drude term. The observation of such infrared features confirms that the cell doubling along the c axis is due to charge ordering. Midinfrared bands similar to those reported here have been observed in other oxides (like nickelates and manganites) which exhibit either commensurate or incommensurate ordering. Therein, however, the Drude term is usually absent below the ordering temperature. In the present cuprate, on the contrary, the ordered charges coexist with carriers moving freely along the c axis, because the two species are probably placed on different paths. In any case, once again the

observation of a T -dependent midinfrared absorption in a cuprate is intimately related to selftrapped, or polaronic, charges, that at high doping may form ordered structures.

We have then studied the ab plane of $\text{La}_{8-x}\text{Sr}_x\text{Cu}_8\text{O}_{20}$, where no indications of superlattice features are extracted from the diffraction experiments. The infrared spectra of the $x = 1.56$ crystal exhibit again both a Drude-like term and a well resolved midinfrared absorption. However the latter band is much softer than for the c axis of the same sample (~ 0.1 eV with respect to 0.3 eV). A fit to the $x = 2.24$ optical conductivity confirms the above two-term scenario also for the highest doping. However, unlike along the c axis, in the ab plane one could have a single type of lightly bound carriers, possibly large polarons. The Drude part of the spectrum would reflect their behavior as quasi-free particles, the soft band at 0.1 eV would correspond to their photoionization, or destruction by the absorption of a photon. This interpretation is strongly supported by the correlation between the T -dependence of the band at 0.1 eV and that of the dc resistivity in the same $x = 1.56$ sample.

By recalling what reported in the Introduction, the ab plane of $\text{La}_{8-x}\text{Sr}_x\text{Cu}_8\text{O}_{20}$, behaves in the infrared like the ab plane of the superconducting cuprates, even if it has a quite different geometrical structure. However, a crucial difference has been pointed out by the present experiment. While in the non- superconducting 8-8-20 the infrared bands related to the bound charges move to higher frequencies for $T \rightarrow 0$, indicating stronger localization, in some high- T_c superconductors the corresponding absorption is found to soften for decreasing temperature in the normal phase, indicating a carrier delocalization or - in a phase separation scenario - stronger charge-density fluctuations. This result should be taken into consideration by those models where the existence of bound charges is related to the elusive phenomenon of high- T_c superconductivity.

ACKNOWLEDGMENTS

We are indebted to M. Capizzi and P. Quemerais for useful discussions and suggestions.

REFERENCES

- ¹ V. J. Emery and S. A. Kivelson, *Physica* (Amsterdam) **209C**, 597 (1993); *Phys. Rev. Lett.* **71**, 3704 (1993).
- ² C. Castellani, C. Di Castro, and M. Grilli, *Phys. Rev. Lett.* **75**, 4650 (1995).
- ³ M. I. Salkola, V. J. Emery, and S. A. Kivelson, *Phys. Rev. Lett.* **77**, 155 (1996).
- ⁴ A. Sadori and M. Grilli, *Phys. Rev. Lett.* **84**, 5375 (2000).
- ⁵ J. Ranninger, *Solid State Commun.* **85**, 929 (1993); J. Ranninger, J. M. Robin, and M. Eschrig, *Phys. Rev. Lett.* **74**, 4027 (1995).
- ⁶ A. Bianconi, A. Valletta, A. Perali, and N. L. Saini, *Solid State Commun.* **102**, 369 (1997).
- ⁷ S. Fratini and P. Quemerais, preprint.
- ⁸ C. H. Chen and S-W. Cheong, *Phys. Rev. Lett.* **76**, 4042 (1996); W. Bao, S-W. Cheong, and W. Chen, *Solid State Commun.* **98**, 55 (1996).
- ⁹ J. M. Tranquada, B. J. Sternlieb, J. D. Axe, Y. Nakamura, and S. Uchida, *Nature* **375**, 561 (1995).
- ¹⁰ H. A. Mook, P. Dai, F. Dogan, and R. D. Hunt, *Nature* **404**, 729 (2000).
- ¹¹ R. P. Sharma, S. B. Ogale, Z. H. Chang, J. R. Liu, W. K. Chu, B. Veal, A. Paulikas, H. Zheng, and T. Venkatesan, *Nature* **404**, 736 (2000).
- ¹² A. Bianconi, N. L. Saini, A. Lanzara, M. Missori, T. Rossetti, H. Oyanagi, H. Yamaguchi, K. Oka, and T. Ito, *Phys. Rev. Lett.* **76**, 3412 (1996).
- ¹³ A. Ino, C. Kim, M. Nakamura, T. Yoshida, T. Mizokawa, Z.-X. Shen, A. Fujimori, T. Kakeshita, H. Eisaki, and S. Uchida, *cond-mat* 9902048.
- ¹⁴ Z. Schlesinger, R. T. Collins, F. Holtzberg, C. Feild, G. Koren, and A. Gupta, *Phys. Rev. B* **41**, 11237 (1990).
- ¹⁵ T. Timusk and B. Statt, *Rep. Prog. Phys.* **62**, 61 (1999).
- ¹⁶ P. Calvani, M. Capizzi, S. Lupi, P. Maselli, A. Paolone, and P. Roy, *Phys. Rev. B* **53**, 2756 (1996).
- ¹⁷ S. Lupi, P. Calvani, M. Capizzi, P. Maselli, W. Sadowski, and E. Walker, *Phys. Rev. B* **45**, 12470 (1992).
- ¹⁸ J. P. Falck, A. Levy, M. A. Kastner, and R. J. Birgenau, *Phys. Rev. B* **48**, 4043 (1993).
- ¹⁹ G. A. Thomas, D. A. Rapkine, S-W. Cheong, and L. F. Schneemeyer, *Phys. Rev. B* **47** (1993) 11369.
- ²⁰ S. Lupi, P. Maselli, M. Capizzi, P. Calvani, P. Giura, and P. Roy, *Phys. Rev. Lett.* **83**, 4852 (1999).
- ²¹ E. J. Singley, D. N. Basov, K. Kurahaschi, T. Uefuji, and K. Yamada, *cond-mat* 0103480.
- ²² S. Lupi, P. Calvani, M. Capizzi, and P. Roy, *Phys. Rev. B* **62**, 12418 (2000).
- ²³ Y. Yagil and E. K. H. Salje, *Physica C* **256** 205 (1996).
- ²⁴ R. P. S. M. Lobo, F. Gervais, and S. B. Oseroff, *Europhys. Lett.* **37**, 341 (1997).
- ²⁵ S. Fratini and P. Quemerais.: *Mod. Phys. Lett. B*, **12** 1003 (1998); *Eur. Phys. J.*, in press.
- ²⁶ V. Cataudella, G. De Filippis, and G. Iadonisi: *Eur. Phys. Journ. B*, **12** 17 (1999).
- ²⁷ J. Tempere and J. T. Devreese, *Phys. Rev. B*, in press.
- ²⁸ J. Tempere and J. T. Devreese, *cond-mat* 0004435 (2000).
- ²⁹ B. Bucher, J. Karpinski, E. Kaldis, and P. Wachter, *it Phys. Rev. B* **45**, 3026 (1992).
- ³⁰ S. Uchida, H. Takagi, and Y. Tokura, *Physica C* **162-164**, 1677 (1989).
- ³¹ S. H. Blanton, R. T. Collins, K. H. Kelleher, L. D. Rotter, Z. Schlesinger, D. G. Hinks, and Y. Zheng, *Phys. Rev. B* **47**, 996 (1993).

³² H. Yamaguchi, H. Matsuhata, T. Ito, and K. Oka, Physica C **282-287**, 1079 (1997).

³³ L. Er-Rakho, C. Michel, and B. Raveau, J. Solid State Chem. **73**, 514 (1988).

³⁴ T. Ito, H. Yamaguchi, K. Oka, K. Nozawa, and H. Takagi, Phys. Rev B **60**, R15031 (1999).

³⁵ T. Ito, H. Yamaguchi, and K. Oka, Chinese Journ. Low Temp. Phys. **19**, 36 (1997).

³⁶ J. Chaussy, P. Haen, J. C. Lasjaunias, P. Monceau, G. Waysand, A. Waintal, A. Meerschaut, P. Molinie, and J. Rouxel, Solid State Commun. **20**, 759 (1976).

³⁷ C. C. Homes, M. Reedik, D. A. Cradles, and T. Timusk, Appl. Optics **32**, 2976 (1993).

³⁸ S. Tajima, H. Ishi, T. Nakahashi, T. Takagi, S. Uchida, M. Seki, S. Suga, Y. Hialaka, M. Suzuki, T. Murakami, K. Oka, and H. Unoki, J. Opt. Soc. Am. **B6**, 475 (1989).

³⁹ X. Bi and P. C. Eklund, Phys. Rev. Lett. **70**, 2625 (1993); Phys. Rev. B **48**, 4043 (1993).

⁴⁰ P. Calvani, A. Paolone, P. Dore, S. Lupi, P. Maselli, P. G. Medaglia, and S-W. Cheong, Phys. Rev. B **54**, R9592 (1996).

⁴¹ D. Emin, Phys. Rev B **48**, 13691 (1993).

⁴² P. Monceau, in *Electronic Properties of Inorganic Quasi-One-Dimensional Compounds*, Part II, D. Reidel Pub. Comp., Dordrech 1985, pp. 139-268.

⁴³ F. Hermann, R. V. Kasowski, and W. Hsu, Phys. Rev. B **37**, 2309 (1998).

FIGURES

FIG. 1. The crystal structure of $\text{La}_{8-x}\text{Sr}_x\text{Cu}_8\text{O}_{20}$ cuprate. The c axis is perpendicular to the sheet. The Cu-O three-dimensional network comes out from the corner-sharing polyhedra. The corner-sharing squares create one-dimensional chains along the c axis.

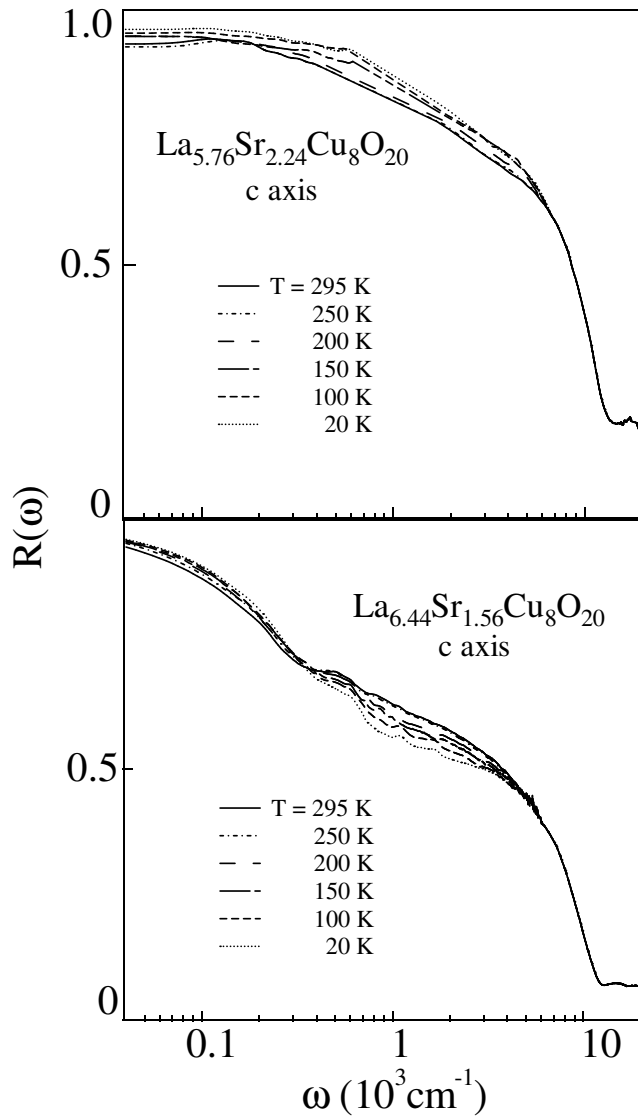


FIG. 2. Infrared reflectivity measured up to 20000 cm^{-1} at different temperatures, with the radiation field polarized along the c axis for both $x = 2.24$ (top) and $x = 1.56$ (bottom).

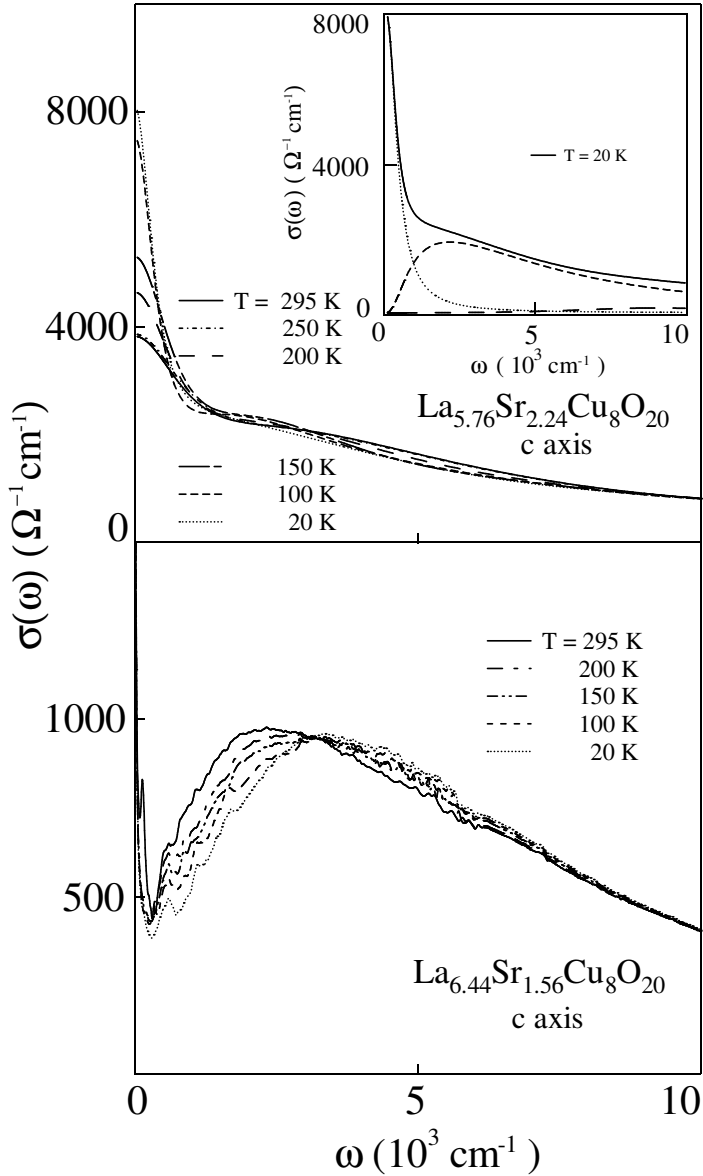


FIG. 3. Infrared optical conductivity of the c axis at different temperatures, as extracted from the $R(\omega)$ of Fig. 2, for $x = 2.24$ (top) and $x = 1.56$ (bottom). The inset compares the experimental $\sigma(\omega)$ at 20 K (solid line) with a fit based on a conventional Drude term (dotted line) and two contributions at infrared frequencies (dashed lines).

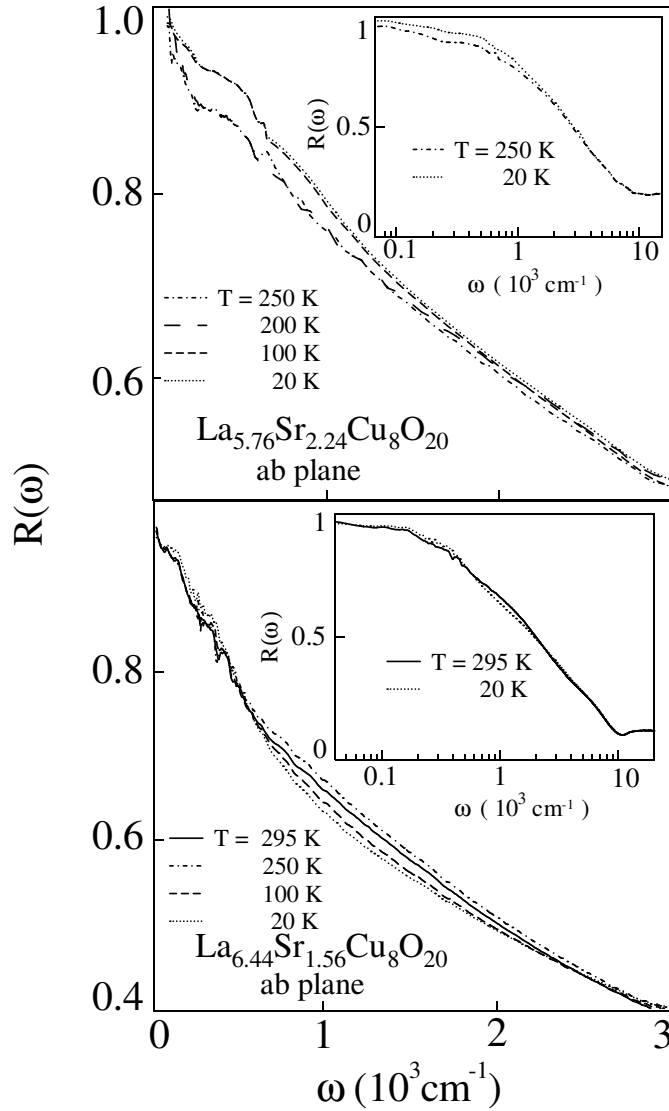


FIG. 4. Infrared reflectivity measured at different temperatures, with the radiation field polarized in the ab plane for both $x = 2.24$ (top), and $x = 1.56$ (bottom). In the insets, $R(\omega)$ is shown at two temperatures up to 20000 cm^{-1} .

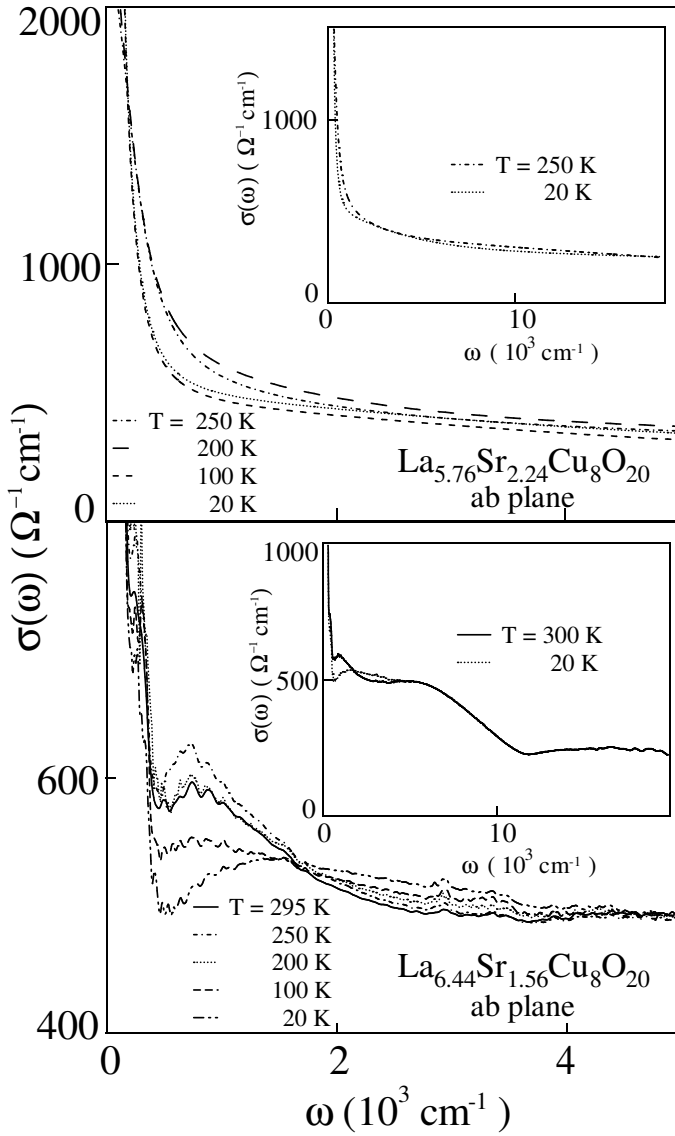


FIG. 5. Infrared optical conductivity in the ab plane, as extracted from the $R(\omega)$ of Fig. 4 at different temperatures. In both insets, $\sigma(\omega)$ is shown in the whole measuring range.

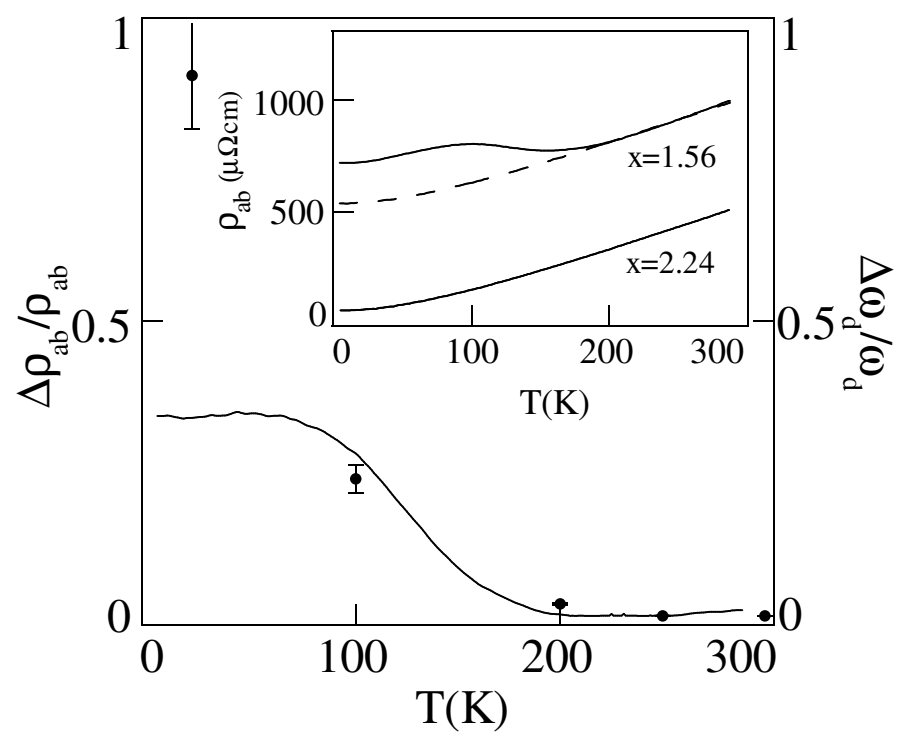


FIG. 6. Behavior with temperature of the ab -plane d band, for $\text{La}_{6.44}\text{Sr}_{1.56}\text{Cu}_8\text{O}_{20}$ compared with that of the dc resistivity ρ_{ab} . Raw ρ_{ab} data are reported in the inset for both $x = 1.56$ and $x = 2.24$ as solid lines. The dashed line is the ρ_{ab} of $x = 2.24$, assumed as a normal metallic reference, once scaled by a constant factor in order to match the high- T ρ_{ab} of $x = 1.56$. In the main Figure, the solid line gives $\Delta\rho_{ab}/\rho_{ab} = [\rho_{ab}(1.56) - \rho_{ab}(2.24)]/\rho_{ab}(2.24)$, namely the deviation of ρ_{ab} in the $x = 1.56$ sample from a normal metallic behavior. The dots represent $\Delta\omega_d/\omega_d = [\omega_d(T) - \omega_d(295)]/\omega_d(295)$, namely the relative "blue shift" of the d band with respect to its room- temperature value.

This figure "Fig1-8820.jpg" is available in "jpg" format from:

<http://arxiv.org/ps/cond-mat/0106402v1>